Supporting information available

Structural details.

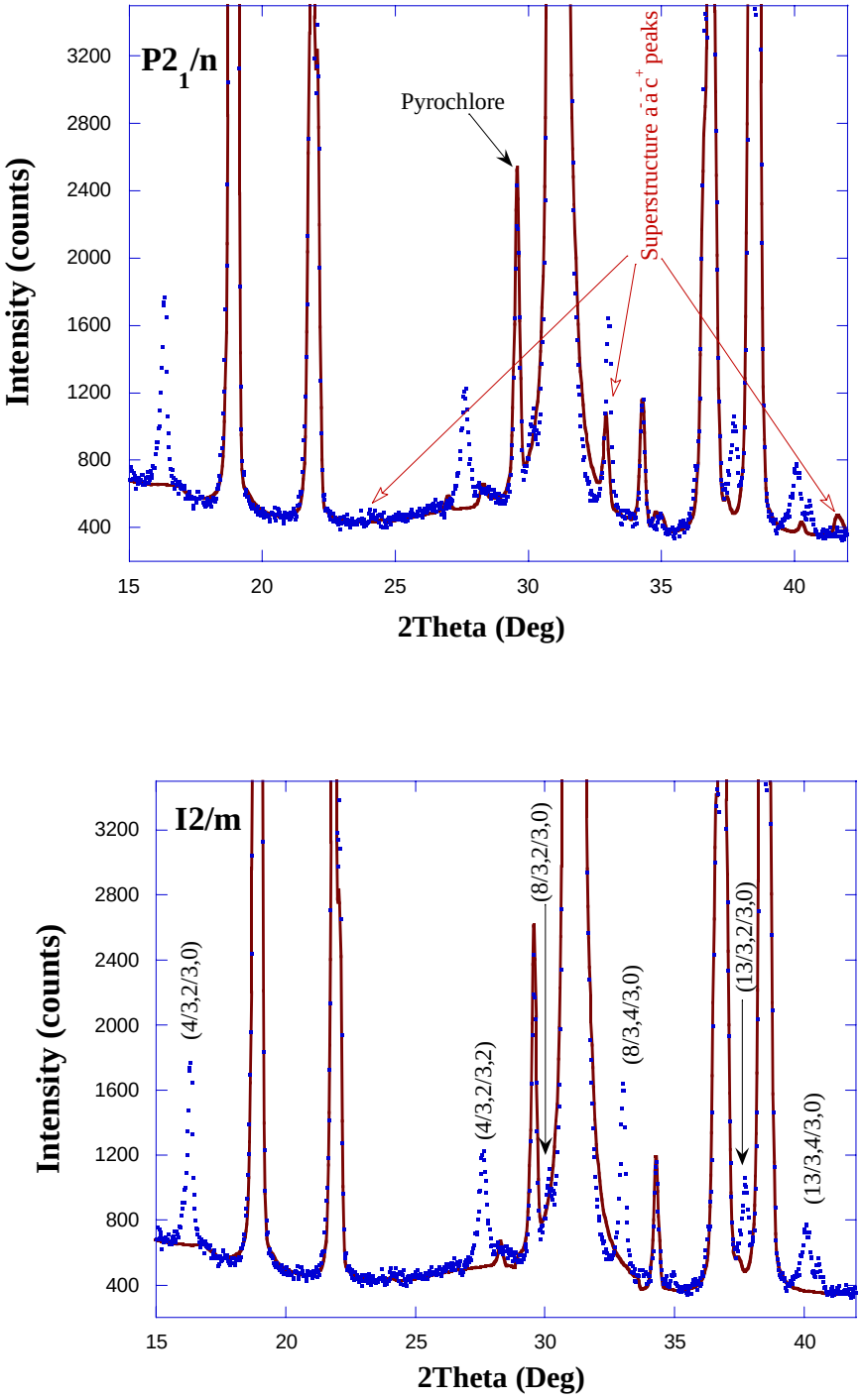

Figure A. Details of the observed (points) and calculated (line) x-ray powder diffraction pattern of Pb_2MnReO_6 at 300 K using the *P2₁/n* and *I2/m* models. The pattern is focused on the region with the main superstructure peaks indexed in the frame of the high-temperature phase. Both monoclinic cells are derived from the parent structure

following the lattice vectors (½, ½, 0), (-½, ½, 0) and (0, 0, 1). The distinction comes from different combination of BO_6 tilts (B=Mn and Re in our case). The refinement in any of the two previous cells yielded similar goodness of the fit with R_{Bragg} values around 6% and 5% for the $P2_1/n$ and $I2/m$ models, respectively. The $P2_1/n$ model presents more superstructure peaks due to the existence of more octahedral tilts. Some of them are not noticeable but the intensity of the visible peaks disagrees with the refined value. This fact explains a larger R_{Bragg} value for the $P2_1/n$ model. Clearly, both models, usually found in double perovskites, fail to reproduce the new superstructure peaks.

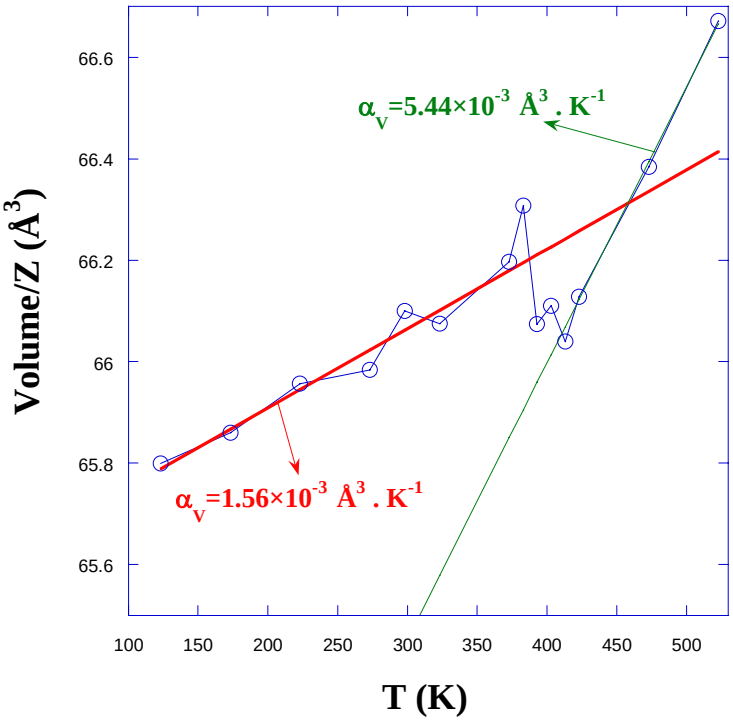

Figure B. Volume per unit formula vs. temperature. Linear fits for each region above and below the transition allow us to extract the average volume expansion coefficients for each phase.

Electrical properties.

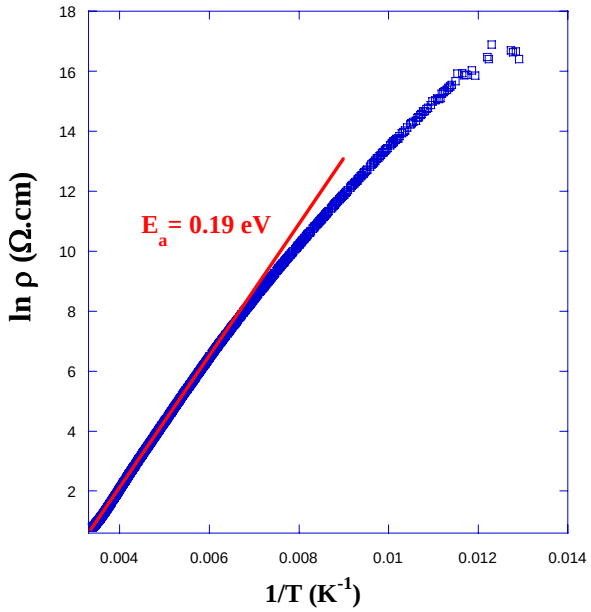

Figure D. Lnρ vs. 1/T at low temperatures. The simple activated behaviour is followed down to ~ 150 K.

Magnetic properties.

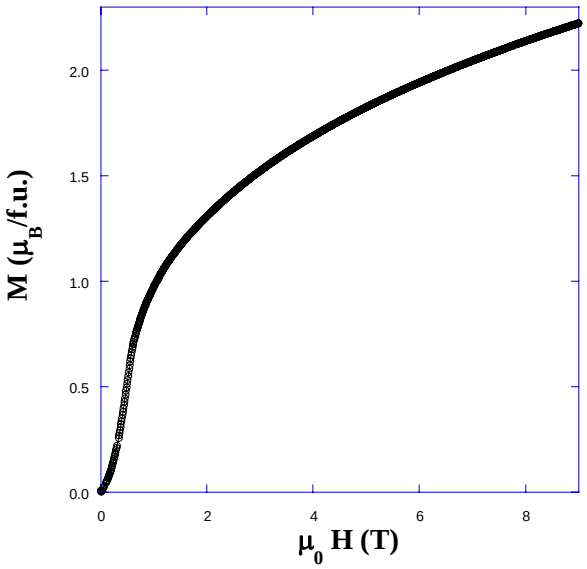

Figure C. Isothermal magnetization at 5 K for Pb_2MnReO_6. The lack of magnetic saturation at fields of 9 T is clear.